Chapter 9
Nanoelectromechanical Systems (NEMS)

Abstract NEMS consist of electronic and nonelectronic components and functions on the nanoscale. These components and functions include sensing, actuation, signal acquisition, and processing. Sometimes display, control, interfacing, and ability to perform chemical and biochemical interactions are also included. NEMS follow both approaches: downscaling previous MEMs components to nanodimensions, and introducing new concepts based on phenomena that are exclusive to nano-regime. Limitations in downscaling are pointed out as well as novel sensing/actuation techniques are presented. NEMS play a critical role in medical diagnostics, displays, energy harvesting, nonvolatile memory, and providing ultra-sharp tips for atomic force microscopy.

9.1 Introduction

Parallel to the relentless march of nanoelectronics toward miniaturization in the "More Moore" sub-domain, the sensing devices too are moving ahead in the "More-than-Moore" roadmap to nanoscale sizes, aiming at the ultimate limits of atoms and molecules. Nanoelectromechanical systems (NEMS) include man-made mechanical elements, sensors, actuators, and signal processing circuits having critical feature sizes between 100 and 1 nm. In NEMS, the mass, thermal capacity, and power consumption decrease as the critical dimension becomes smaller. Contrarily, the fundamental frequency, mass/force sensitivity, and quality or Q-factor increase as the critical dimension is reduced. Present technology has enabled the fabrication of NEMS of masses $\sim 10^{-18}$ g and cross-sectional area ~ 10 nm $\times$ 10 nm. By virtue of infinitesimally small sizes, NEMS have achieved frequencies ~ 100 GHz, Q-factors $\sim 10^3$–10^5 in moderate vacuum [1], force sensitivities $\sim 10^{-18}$ N, thermal capacities $\sim 10^{-24}$ cal, power consumption $\sim 10^{-18}$ W, integration density $\sim 10^{12}$ elements cm^{-2}, and ultra-low mass sensitivities up to molecular level [2]. These unique characteristics of NEMS strikingly differ from those of their predecessor MEMS. In comparison to MEMS, NEMS combine smaller mass with

V.K. Khanna, *Integrated Nanoelectronics*,
NanoScience and Technology, DOI 10.1007/978-81-322-3625-2_9

higher surface-area-to-volume ratio to achieve better sensitivities. Constructional materials for NEMS are silicon, silicon carbide, CNTs, Au, Pt, etc.

9.2 NEMS Sensor Classification

NEMS sensors are compartmentalized into two parts: (i) MEMS sensors that have been downscaled to nano–dimensions; and (ii) novel nanosensors and systems that have been developed especially for nanoscale, e.g., CNT-based. These sensors are unique to the nanodomain. They are required because several MEMS sensors cannot be downscaled due to restrictions imposed by noise and sensitivity. So, they cannot provide the desired resolution in their nano-versions. Further, many microsensors cannot be fabricated in nanosensor form due to technological problems. Therefore, downscaling fails. The metric used for measuring the performance of downscaled sensor is the ratio of the range of measurand to the resolution of the readings. This ratio is known as the dynamic range of the sensor [3].

9.3 MEMS Sensors Downscalable to NEMS Version

9.3.1 Piezoresistive Sensors

Piezoresistance is a basic material property in the toolbox of sensor design engineers. Piezoresistive sensors are used to measure displacement/force/pressure from the change in resistance of a piezoresistor formed on a cantilever beam [4] at the point of flexure. The cantilever, a beam fixed at one end and free at the other end, is a ubiquitous sensing element in the realm of micromachined devices (Fig. 9.1).

The piezoresistance change is caused by the surface stress generated in the cantilever beam on bending. The change in surface stress Δg resulting from deflection Δh of the cantilever is expressed by Stoney's formula [5]

$$\Delta g = [E\Delta h/\{4(1-v)\}](t/L)^2 \tag{9.1}$$

where E and v are the Young's modulus and Poisson's ratio of cantilever material; t and L denote the thickness and length of the cantilever beam.

Piezoresistive sensors are also used to determine pressure from resistance changes of a piezoresistor made in monocrystalline silicon or polysilicon film deposited at the peripheral regions on a circular or rectangular diaphragm subjected to pressure [6], Fig. 9.2. By anisotropically etching silicon from the backside, a cavity is formed terminating near the surface of the silicon to form a circle-/rectangle-shaped

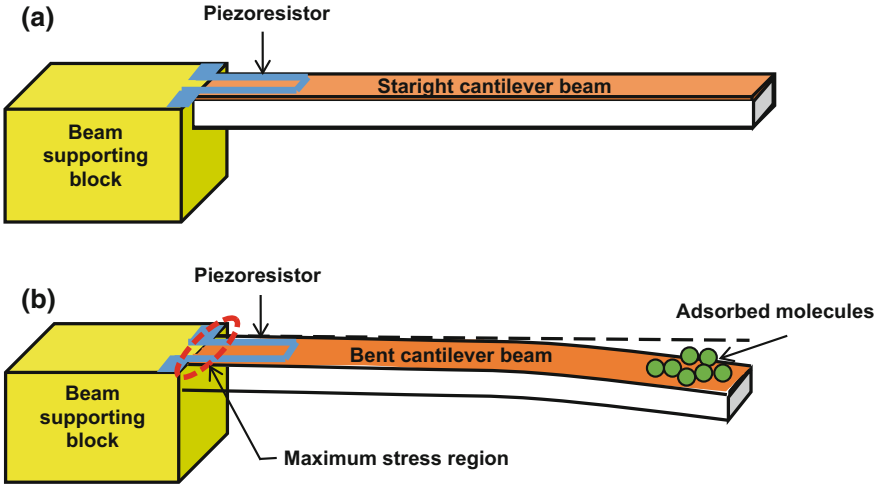

Fig. 9.1 Nanocantilevers: **a** straight and **b** bent by the mass of adsorption of molecules

diaphragm of required thickness [7]. A pressure applied on the diaphragm such as by a fluid produces mechanical tension at its edges. Piezoresistors are positioned at the locations of highest tension to achieve maximum sensitivity. Two resistors are placed such that current flows in a direction parallel to that of tension. The other two resistors are placed in such a way that current flows perpendicular to the direction of tension. The resistor areas are doped with ion implantation to get the desired resistance values. Through aluminum metallization film, the piezoresistors are connected together in a Wheatstone bridge configuration.

The sensor is susceptible to Flicker noise and Johnson noise. When it is decreased in size, flicker noise becomes dominant. The dynamic range is restricted to <60 dB.

9.3.2 Tunneling Sensors

They comprise a sharp tip in vicinity of a moving surface. As the tip is raster scanned over the surface, the tunneling current varies with distance between the tip and the surface providing high displacement sensitivity. The variation of tunneling current i with the distance d separating the tip and the surface is given by

$$i = \rho_S(E_F)V\exp(-2\pi\lambda d) \tag{9.2}$$

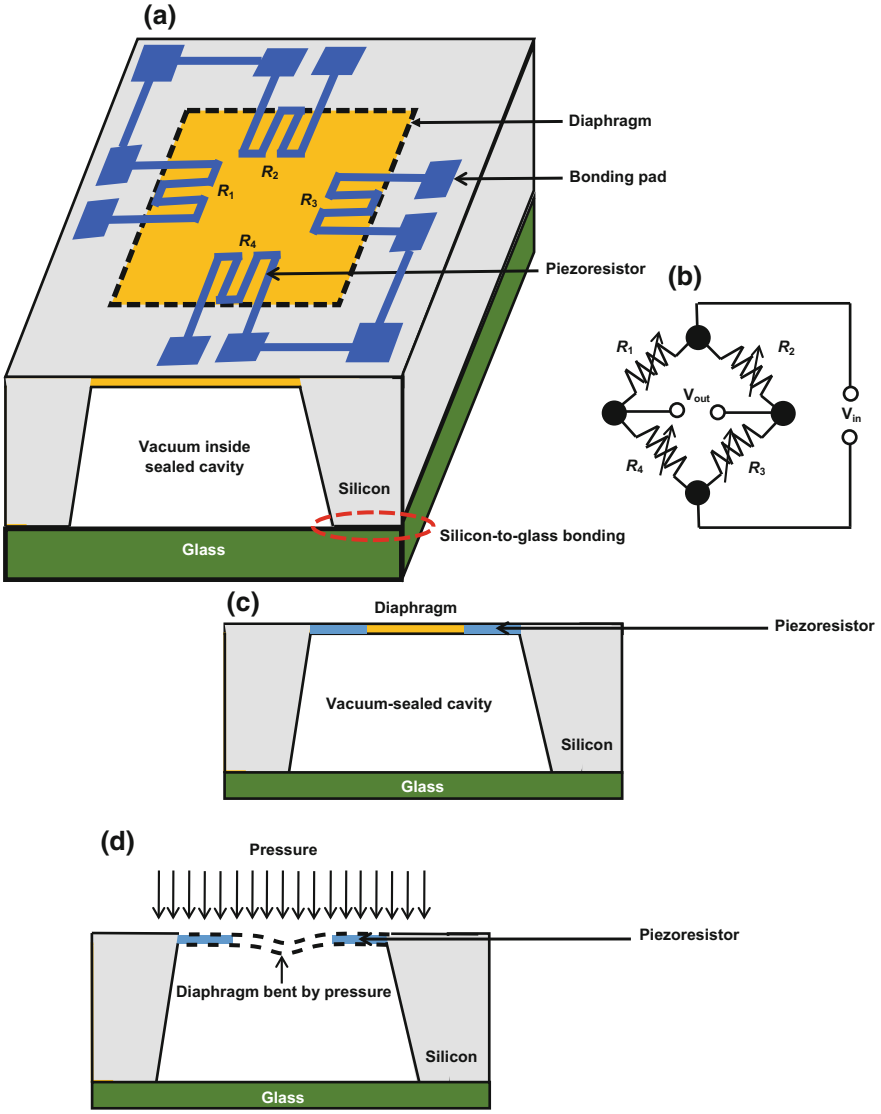

Fig. 9.2 Absolute pressure sensor: **a** 3-D view of pressure sensor chip bonded on glass; **b** wheatstone bridge connection of piezoresistors on the diaphragm; **c**, **d** cross-sectional diagrams showing straight and bent diaphragms

where V is the applied DC voltage, $\rho_S(E_F)$ is the density states of electrons localized around the tunneling region, E_F is the Fermi level, and λ is the decay constant of the electron wave function in the tunneling gap.

Their range and resolution do not downscale as the size decreases, making them ideally suited to nanorange.

9.4 MEMS Sensors Not Downscalable to NEMS Version

Piezoelectric sensors are active sensors, which use a film of a piezoelectric material such as ZnO or PZT deposited on a diaphragm or a clamped–clamped beam to measure vibrations or accelerations. They show a diminution in dynamic range with sensor size. Capacitive sensors use parallel-plate or comb drive configurations to detect out-of-plane/in-plane motion in accelerometers or gyroscopes. They do not work at all at nanoscale because their dynamic range decreases with size. Problem with Hall effect sensors used for measuring displacements is the interference from stray magnetic fields.

9.5 CNT-Based Piezoresistive Nanosensors

These sensors have intrinsically nanosizes. They provide large gauge factors and hence are capable of >60 dB dynamic range at a footprint of 1 μm × 1 μm. CNT sorting technique needs to be perfected so that CNTs of highest gauge factor can be employed for sensor fabrication.

Figure 9.3 shows the schematic diagram of a pressure sensor using SWCNT as the sensitive element. An SWCNT was adsorbed on the surface of an alumina membrane of thickness 100 nm [8]. Source and drain leads were connected to the SWCNT for electrical measurements. The membrane was circular in shape with a diameter of 50–100 μm. It was formed by bulk micromachining. For SWCNTs with metallic behavior, the piezoelectric gauge factor was found to be 210.

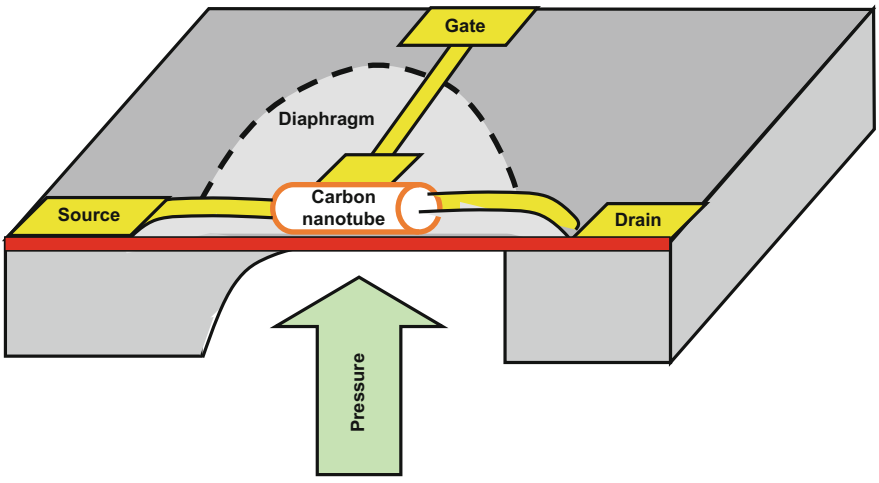

Fig. 9.3 CNT pressure sensor

9.6 NEMS Resonators

These are cantilevers or doubly clamped beams (Fig. 9.4). They have a miniscule mass. They dissipate very little power leading to extremely high quality factors. Their resonance frequency is inversely proportional to mass and to square of length of the device. It is very high >1 GHz, thereby enhancing the sensitivity as well as speed of signal processing.

Graphene nanoribbon has been used as a doubly clamped beam resonator (Fig. 9.5).

9.6.1 Resonator-Based Mass Sensors

Addition of a small mass to the resonator cases a shift in its resonance frequency, which is directly proportional to the incremental mass. The sensitivity of detection is given by

$$\Delta f_r/\Delta m = (1/2m)f_r \tag{9.3}$$

where Δf_r is the change in resonance frequency f_r when an extra mass Δm is added to the original mass m. Here, $\Delta m \ll m$. This equation shows that the sensitivity

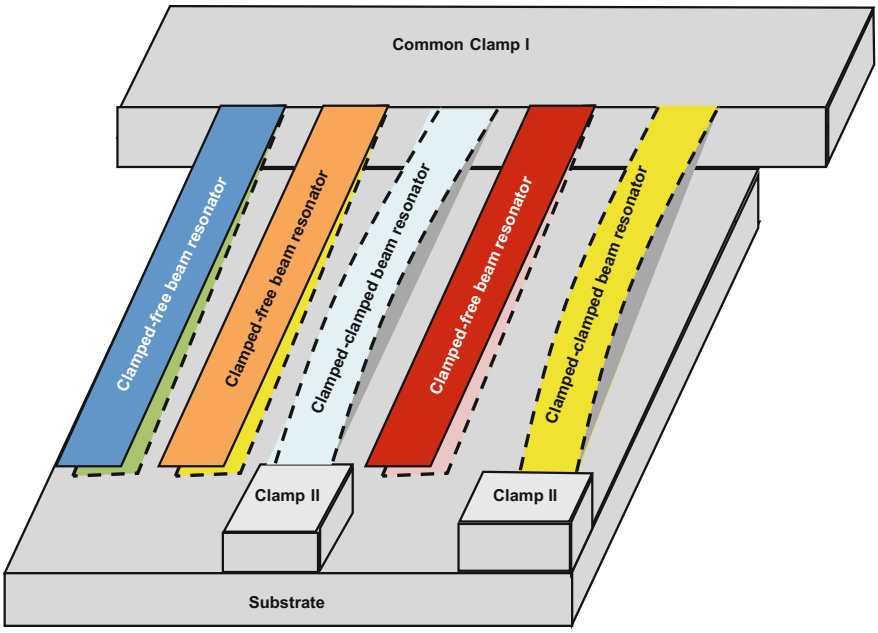

Fig. 9.4 Two types of resonators: singly clamped beam (cantilever) and doubly clamped beam

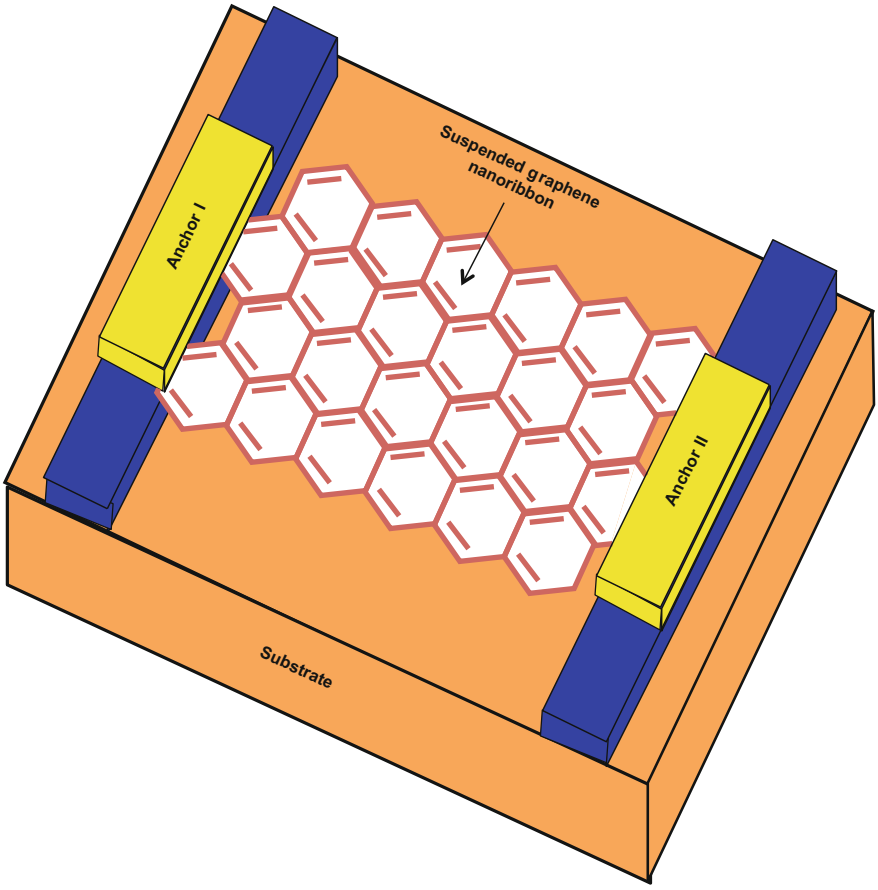

Fig. 9.5 Graphene nanoribbon as a NEMS resonator

increases with increase in resonance frequency. Hence, ultrahigh frequencies are needed for detecting very small masses. NEMS-based mass spectrometry has rendered possible detection of protein molecules and nanoparticles in real time immediately on their adsorption on the sensor [9].

Masses up to 10^{-18} g have been measured using silicon nanocantilevers or beams clamped on both sides. CNT-based resonators are capable of 10^{-21} g resolution. The NEMS resonators are prone to thermomechanical noise, limiting their dynamic range to 60 dB.

The resonant sensors have been utilized as a platform whose surface is functionalized for detection of gases or biomolecules. CNTs with carboxylic chloride groups were used for NO_2 detection [10].

9.6.2 Resonator-Based Strain Sensors

On subjecting a clamped–clamped flexure beam to tension, the beam increases in length. Tension makes the beam stiff and unbending. The stiffness of the beam causes a change in its natural frequency. This change in frequency is correlated to the strain. CNTs are very useful in these devices due to their high modulus of elasticity and large strength [11]. For similar reasons, graphene-based NEMS resonators are also promising [12].

9.7 NEMS Actuators

In NEMS applications, particularly for optical and RF systems, MEMS actuation reduces both speed and accuracy. So, suitable NEMS actuators offering nanoscale precision must be provided. Nanoactuation is actuation of a function using a nanosize object.

9.7.1 CNT Nanotweezers

Nanotweezers consist of two arms of CNTs [13]. These arms are fixed on a silicon tip with metal electrodes. For this fixation, viewing was done through SEM. On applying a DC voltage between the two CNTs, they move toward each other. The nanotweezers are operated electromechanically for manipulating nanomaterials in scanning probe microscopes such as STM (scanning tunneling microscope) and AFM (atomic force microscope).

9.7.2 Nanogrippers

A nanogripper or ‘robotic hand for ultra-small objects’ is a ‘pick-and-place’ device with two end effectors consisting of a nanotip made from a tungsten tip and CNT [14]. These end effectors can be used to apply forces acting in opposite directions on nanoscale objects to grasp them, lift them up from their positions, hold them, and place them, as desired. Nanogrippers have been fabricated whose arms can be opened/closed by electrostatic actuation that can also measure the size of the specimen [15]. Electrothermal actuation has been exploited in silicon nanogrippers to make them expand [16].

9.7.3 Magnetic Bead Nanoactuator

A titanium cantilever carries a bead made of a superparamagnetic material at its front end. The deflection of the cantilever can be controlled by an externally applied magnetic field gradient [17]. Superparamagnetism is a type of magnetism found in ferromagnetic/ferrimagnetic nanoparticles. It is the property by which the direction of magnetic moments changes in some materials at nanoscale and they behave like a paramagnet even below Curie temperature without applying any magnetic field. At the same time they show a high magnetic susceptibility like a ferromagnetic material, i.e., exhibit a high degree of response to an applied magnetic field.

9.7.4 Nanoactuation by Magnetic Nanoparticles and AC Fields

22-nm-size magnetic nanoparticles were injected into the brain tissue [18]. The neurons were excited by triggering thermally sensitive capsaicin receptors by applying an alternating electric field externally. By this method, calcium ions were introduced into neurons.

9.7.5 Ferroelectric Switching-Based Nanoactuator

When the electric field is absent, the nanoactuator is in the ground state in which the domains are polarized [19]. On applying an electric field, the polarization undergoes reorientation. Strain is thus produced. As soon as the electric field is withdrawn, the nanoactuator once again reverts back to the ground state. Thus a repeatable actuation cycle is completed.

9.7.6 Optical Gradient Force-Driven NEMS Actuator

Optical gradient force can produce mechanical deformation in the nano-regime [20]. This force is appreciably stronger in evanescently coupled waveguides owing to the larger value of the gradient of optical field intensity. Use of ring resonator of high quality factor increases the optical field intensity by many orders of magnitude, enhancing the force still further, and enabling its exploitation for nanoactuation. The nanoactuator, drawn according to Dong, consists of three main components (Fig. 9.6): (i) An actuation ring resonator: Its Q-factor is controlled by P–I–N electro-optics modulator. The rib waveguide forms a part of this resonator. The slab on one side is doped with P-type and that on the other side is doped with N-type

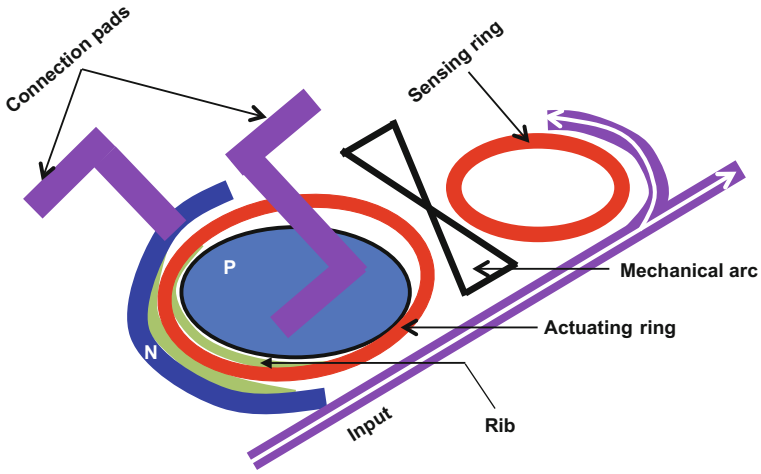

Fig. 9.6 Components of optical gradient actuator

constituting a P–I–N junction. The modulator induces free carriers into the actuation resonator to alter its absorption coefficient for changing the *Q*-factor. (ii) A sensing ring resonator: It measures the actuation displacement. It is optically linked with the actuation resonator. (iii) A mechanical arc: Optical gradient force is produced between the actuation resonator and the mechanical arc.

On changing the *Q*-factor of the ring resonator from 15000 to 6000, the actuation displacement reached 14 nm. The actuator can be applied to manipulating single molecules and sensors of high sensitivity.

9.8 NEMS Memories

These are memories utilizing NEMS switches to reduce leakage currents [21]. They provide high ON/OFF ratios $\sim 10^5$. Further, they can function in hostile environments such as at elevated temperatures and in radiation-polluted spaces. Different architectures consisting of two or three electrodes have been conceived. One common two-electrode architecture consists of a TiN cantilever/a hanging bridge and a stationary TiN/W electrode at a separation of 15–20 nm (Fig. 9.7a). Voltage applied between the two electrodes activates the switching action for closing or opening of the switch leading to its on and off states. In the suspended bridge structure, the top electrode anchored on an insulating support is mobile while the bottom electrode is static (Fig. 9.7b).

Another electrode architecture comprises crossed pairs of CNTs (Fig. 9.8). One pair of parallel CNTs running on an Si/SiO_2 substrate is connected to metal electrodes A and B. A second pair of parallel CNTs moves perpendicular to the first

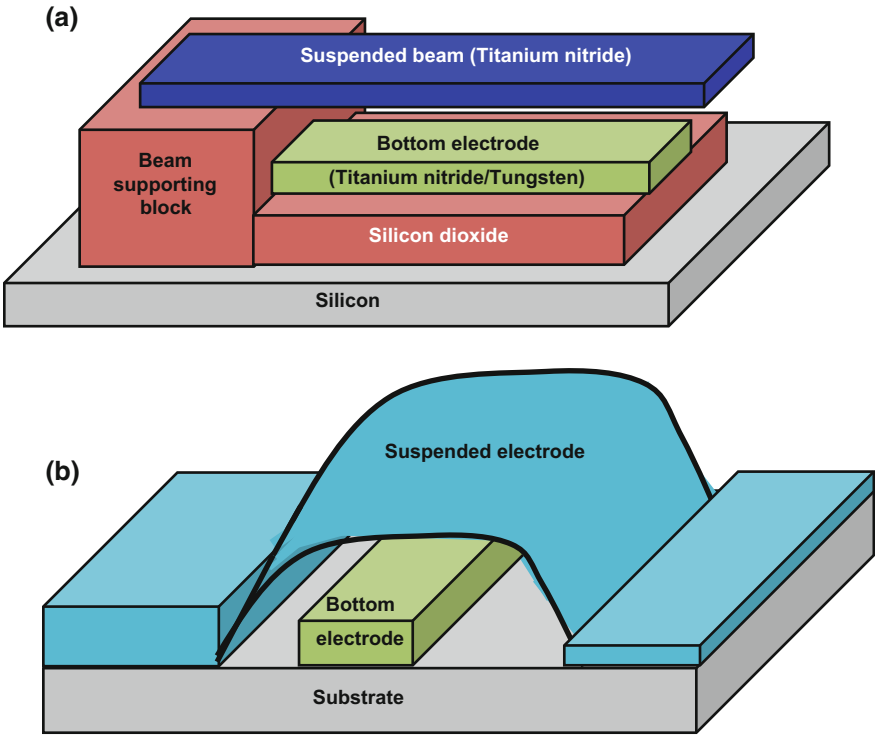

Fig. 9.7 Two electrode architectures using **a** cantilever and **b** suspended bridge

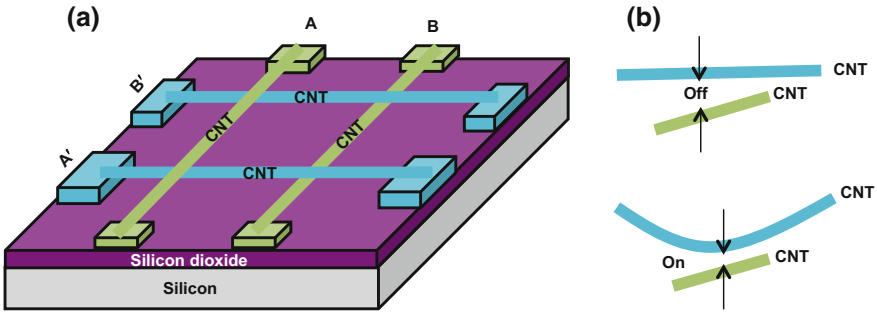

Fig. 9.8 CNT arrangement and disposition: **a** perpendicularly placed pairs of CNTs, **b** their disposition in off and on states

pair, and is connected to metal dots A′ and B′. The gap intervening the two CNT pairs at their intersection is very small ~ 1 nm or less. The on and off states are distinguished from the magnitude of tunneling currents between the two pairs.

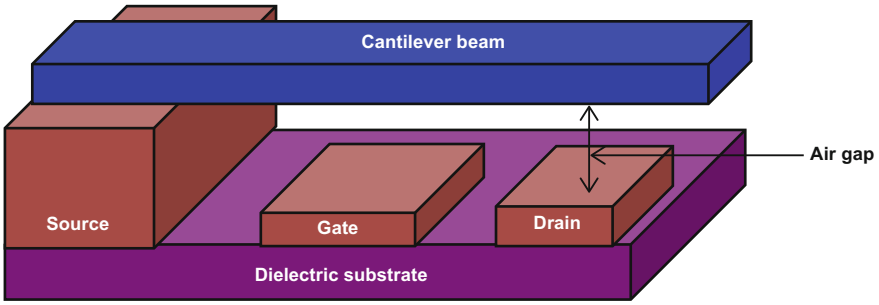

Fig. 9.9 Capacitive three-electrode structure

In the three-electrode architecture, a third motionless top electrode controls the motion of the cantilever/suspended bridge like the gate electrode of a field-effect transistor (FET), Fig. 9.9.

9.9 Discussion and Conclusions

A plethora of nanosensors and nanoactuators were described. NEMS components outperform their MEMS competitors in speed and resolution. They have established superiority due to their small sizes and abilities to execute tasks, which are impossible for MEMs devices. Such tasks include their placement inside the human body to provide medical diagnostic information in real time.

Review Exercises

9.1. What are NEMS? Name some materials commonly used in fabrication of NEMS. Compare NEMS with MEMs.
9.2 How does the reduction of critical feature size affect the following: (i) power consumption, and (ii) Q-factor?
9.3 What are the two sub-classes of NEMs sensors? What is the basis of this classification? Name and define the figure of merit to assess the performance of a downscaled sensor.
9.4 Write Stoney's formula of surface stress. Explain the symbols used.
9.5 At what locations are the piezoresistors placed for maximum sensitivity on (i) a cantilever, and (ii) a diaphragm? Explain the working of a piezoresistive pressure sensor.
9.6 What types of noises is a piezoresistor susceptible to? How do these noises impact the performances of piezoresistive sensors when their sizes are reduced to nanoscales?

9.7 How does the tunneling current vary as a function of distance between the electrode tip and the scanned surface? What makes tunneling sensors ideal for nanoscale?
9.8 Name three categories of MEMs sensors which do not perform well at nanodimensions. Enumerate the reasons for this behavior.
9.9 What are the merits of CNT-based piezoresistive sensors? Explain with a diagram the operation of a pressure sensor using SWCNT.
9.10 What is a NEMS resonator? How does its sensitivity vary with its resonance frequency?
9.11 Write the equation relating the incremental mass placed on a NEMS resonator and the shift in its resonance frequency? Can this device be applied to mass spectrometry?
9.12 What is a nanotweezer? How is it made and how is it used to manipulate nanomaterials?
9.13 What is a magnetic bead nanoactuator? How does it function?
9.14 Explain with a diagram the operation of an optical gradient force-driven nanoactuator? What is the typical range of displacement achieved by Q-factor modulation?
9.15 What are the advantages of NEMS memories? Describe the different two-electrode architectures used for switching between on and off states? How does the three-electrode architecture resemble an FET?

References

1. Roukes ML (2000) Nanoelectromechanical systems. Technical digest of the 2000 solid-state sensor and actuator workshop, Hilton Head Isl., SC, 6/4-8/2000, pp 1–10
2. Mukherjee S, Aluru NR (2006) Preface: Applications in micro- and nanoelectromechanical systems. Eng Anal Boundary Elem 30:909
3. Cullinan MA, Panas RM, DiBiasio CM et al (2012) Scaling electromechanical sensors down to the nanoscale. Sens Actuators, A 187:162–173
4. Li M, Tang HX, Roukes ML (2007) Ultra-sensitive NEMS-based cantilevers for sensing, scanned probe and very high-frequency applications. Nat Nanotechnol 2:114–120
5. Datar R, Kim S, Jeon S et al (2009) Cantilever sensors: Nanomechanical tools for diagnostics. MRS Bull 34:449–454
6. Barlian AA, Park W-T, Mallon JR Jr et al (2009) Review: semiconductor piezoresistance for microsystems. Proc IEEE Inst Electr Electron Eng 97(3):513–552
7. Maxim integrated: Application Note 871, Demystifying piezoresistive pressure sensors, Jul 17, 2002, pp 1–12. http://pdfserv.maximintegrated.com/en/an/AN871.pdf. Accessed 19 Sept 2015
8. Stampfer C, Helbling T, Obergfell D et al (2006) Fabrication of single-walled carbon-nanotube-based pressure sensors. Nano Lett 6(2):233–237
9. Naik AK, Hanay MS, Hiebert WK et al (2009) Towards single-molecule nanomechanical mass spectrometry. Nat Nanotechnol 4:445–450
10. Cobiano C, Serban B, Petrescu V et al (2010) Towards nanoscale resonant gas sensors. Ann Acad Rom Scientists 3(2):39–60
11. Cao G, Chen X, Kysar J (2005) Strain sensing of carbon nanotubes: numerical analysis of the vibrational frequency of deformed single-wall carbon nanotubes. Phys Rev B 72:195412

12. Lee C, Wei X, Kysar JW et al (2008) Measurement of the elastic properties and intrinsic strength of monolayer graphene. Science 321:385–388 (New York)
13. Akita S, Nakayama Y (2002) Manipulation of nanomaterial by carbon nanotube nanotweezers in scanning probe microscope. Jpn J Appl Phys 41:4242–4245
14. Lee J, Kwon S, Choi J et al (2004) Nanogripper using carbon nanotube. NSTI-Nanotech 3:180–182
15. Konno T, Hayashi H, Tan T et al (2006) US 20060220659 A1: Nanogripper device having length measuring function and method for length measurement executed with nanogripper device having length measuring function
16. Berger M (2008) Nanotechnology gets a grip Copyright Nanowerk LLC. http://www.nanowerk.com/spotlight/spotid=8390.php. Accessed 20 Sept 2015
17. Hartbaum J, Jakobs P, Wohlgemuth J et al (2012) Magnetic bead nanoactuator. Microelectron Eng 98:582–586
18. Nanotherics: nano actuation: using magnetic nanoparticles and AC magnetic fields in neurological and biomedical applications, Updated September 10, 2015. http://www.azonano.com/article.aspx?ArticleID=4130. Accessed 20 Sept 2015
19. Balakrishna AR, Huber JE, Landis CM (2014) Nano-actuator concepts based on ferroelectric switching. Smart Mater Struct 23(8):085016 (8 pp)
20. Dong B, Cai H, Ng GI et al (2013) A nanoelectromechanical systems actuator driven and controlled by *Q*-factor attenuation of ring resonator. Appl Phys Lett 103:181105-1–181105-5
21. Lacaze PC, Lacroix J-C (2014) Volatile and non-volatile memories based on NEMS, in non-volatile memories. John Wiley & Sons, Inc., Hoboken, NJ, USA. doi: 10.1002/9781118789988.ch4